Statistical Analysis of Energization Overvoltages in EHV Hybrid OHL-Cable Systems

Khalilnezhad, Hossein; Popov, Marjan; Sluis, Lou van der; Bos, Jorrit A.; Ametani, Akihiro

DOI
10.1109/TPWRD.2018.2825201

Publication date
2018

Document Version
Final published version

Published in
IEEE Transactions on Power Delivery

Statistical Analysis of Energization Overvoltages in EHV Hybrid OHL–Cable Systems

Hossein Khalilnezhad, *Graduate Student Member, IEEE*, Marjan Popov, *Senior Member, IEEE*, Lou van der Sluis, *Life Senior Member, IEEE*, Jorrit A. Bos, and Akihiro Ametani, *Life Fellow, IEEE*

***Abstract*—Energization overvoltages are among the severest overvoltages stressing insulations of EHV power system components. Since these overvoltages have a statistical nature, the insulation level should be determined with the use of a statistical approach by which the distribution of overvoltages is calculated. Literature has properly studied the distribution of energization overvoltages in purely overhead line (OHL) or cable systems, but such a study is not available for hybrid systems consisting of both OHLs and cables. It is expected that the overvoltage distributions change substantially when both OHLs and cables are used in a transmission line. This paper tackles this issue by analyzing the overvoltage distributions due to the energization of a 380 kV hybrid OHL-cable circuit, in which the cable length is variable. The study includes various sensitivity analyses to find out the impact of system parameters and topology on overvoltages. By the statistical analysis, it has been discovered that energization overvoltages of a hybrid OHL–cable circuit are higher than those of a fully-cable circuit and very likely lower than those of a fully-OHL circuit with the same transmission lengths.**

***Index Terms*—Cables, energization overvoltages, insulation coordination, switching transients, statistical analysis.**

I. Introduction

POWER transmission systems have been traditionally developed mainly by the use of overhead lines (OHLs). However, with the increasing tendency in the application of EHV underground cables, future grids will be composed of OHLs and cables combined. These grids are known as hybrid OHL-Cable transmission systems.

The transient behavior of a hybrid OHL-Cable system is significantly different from an OHL-based system due to substantial differences between electrical characteristics of OHLs and cables. As a result, several questions have been raised concerning the technical operation and reliability of hybrid grids [1], [2]. A very important question is how the statistical distribution of energization overvoltages would be in hybrid systems and which parameters can affect their significance.

The determination of the statistical distribution of energization overvoltages is highly recommended for insulation coordination studies due to the statistical nature of switching actions and the insulation strength. The risk of an insulation failure can be calculated by the comparison of the overvoltage probability distribution and the insulation breakdown probability distribution [3]–[5].

The statistical nature of energization overvoltages is the result of the random behavior of the circuit-breaker closing time. The breaker contacts can be switched at any point on the voltage waveform with a pole closing span. The pole closing span is the time difference between the first and the last pole to close due to different stochastic variations in the operating time of each pole [6], [7].

The detailed study of the statistical distribution of line energization overvoltages (OHL or cable) are addressed in [8]–[17]. In [12], [13], the statistical distribution of energization overvoltages in EHV cables and OHLs are compared, where it is concluded that overvoltages in a cable line are lower than those in an OHL. However, despite the importance of the issue, there is very limited literature related to the statistical switching analysis of hybrid circuits consisting of OHLs and cables combined.

It is reported in [18] that energization overvoltages in a cable system are in general lower than those in an OHL-Cable system. In [19], authors concluded that energization overvoltages of a hybrid OHL-Cable circuit are lower than those in a purely OHL circuit and higher than those in a purely cable circuit. However, these conclusions cannot be generalized as the mentioned studies ignore the breaker pole span and also they are only for one circuit topology and one set of system parameters.

A more comprehensive study is required for hybrid systems where the impacts of various system topologies and parameters are investigated; most notably, the cable length, configuration of the hybrid OHL-Cable circuit, short cable sections, and system short-circuit power. In practice, the distribution of overvoltages can be significantly different from one system to another and this can be identified by a sensitivity analysis.

The aim of this paper is to address the mentioned crucial scientific gaps and perform sensitivity analyses on system parameters to investigate the statistical distribution of transient energization overvoltages in hybrid OHL-Cable circuits. In addition,

Manuscript received November 2, 2017; revised February 27, 2018; accepted March 24, 2018. Date of publication April 9, 2018; date of current version November 20, 2018. This work was supported in part by TenneT TSO B.V., Arnhem, The Netherlands, within the framework of the 380 kV cable research program. Paper no. TPWRD-01331-2017. *(Corresponding author: Hossein Khalilnezhad.)*

H. Khalilnezhad, M. Popov, and L. van der Sluis are with the Delft University of Technology, Delft 2628CD, The Netherlands (e-mail: H.Khalilnezhad@tudelft.nl; M.Popov@tudelft.nl; L.vandersluis@tudelft.nl).

J. A. Bos is with TenneT TSO B.V, Arnhem, 7186800, The Netherlands (e-mail: Jorrit.Bos@tennet.eu).

A. Ametani is with Doshisha University, Kyoto 610-0321 Japan (e-mail: aametani@mail.doshisha.ac.jp).

Color versions of one or more of the figures in this paper are available online at http://ieeexplore.ieee.org.

Digital Object Identifier 10.1109/TPWRD.2018.2825201

TABLE I
CABLE SCENARIOS FOR THE HYBRID OHL-CABLE CIRCUIT

Scenario	Total transmission length (km)	
	OHL	Cable
0% Cable (Fully OHL)	80	0
15% Cable	68	12
25% Cable	60	20
50% Cable	40	40
75% Cable	20	60
100% Cable (Fully Cable)	0	80

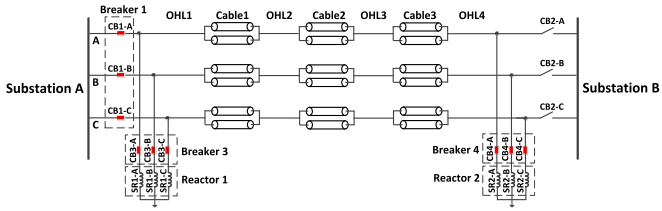

Fig. 1. Study case mixed-line configuration with LEC.

overvoltages due to the presence of trapped charges in the cable are also studied.

II. STUDY CONSIDERATIONS

To ensure the comprehensiveness and preciseness of the study, a wise approach of modelling and simulation had to be considered to drive the statistical distribution of energization overvoltages in hybrid OHL-Cable systems.

A. Cable Scenarios

Six cable scenarios were defined to determine the influence of the cable length on the distribution of energization overvoltages in hybrid circuits. In each scenario, it is specified how many kilometers of the total transmission length is realized by cables. The total transmission length of the hybrid circuit under study is 80 km from the sending substation to the receiving substation. By these scenarios, the cable share varies from 0% (fully OHL) to 100% (fully cable) of the transmission length. The cable scenarios are presented in Table I.

B. Mixed-Line Configuration

A hybrid OHL-Cable circuit is composed of solidly series-connected OHL and cable sections. Mixed-line is the term that is usually used to refer to these circuits. The configuration of a mixed-line is determined by the number and location of OHL and cable sections, which can be decided in the planning and design stages of hybrid circuits.

Fig. 1 shows the study case mixed-line configuration of this paper. The circuit has four OHL sections and three cable sections, where the cable sections are composed of two parallel cables per phase to achieve the same transmission capacity as the OHL sections.

The three-phase shunt reactors for reactive power compensation are connected to the circuit at the two remote ends (right behind the line breakers) through their own breakers (breakers 3 and 4). This type of compensation is known as line-end compensation (LEC).

TABLE II
TRANSMISSION LENGTHS OF OHL AND CABLE SECTIONS IN EACH CABLE SCENARIO

Scenario	Section length (km)						
	OHL 1	Cable 1	OHL 2	Cable 2	OHL 3	Cable 3	OHL 4
15% Cable	5	2	21	5	28	5	14
25% Cable	4	4	20	7	24	9	12
50% Cable	2	13	13	17	14	10	11
75% Cable	0	22	8	18	7	20	5

TABLE III
REQUIRED SHUNT COMPENSATION SIZE FOR EACH CABLE SCENARIO

Scenario	Compensation size (Mvar)		
	SR1	SR2	K_{Sh}
15% Cable	88	88	69.8%
25% Cable	178	178	84.8%
50% Cable	375	375	89.3%
75% Cable	580	580	92.1%
100% Cable (Fully Cable)	800	800	95.2%

The connection of shunt reactors to the circuit helps to limit energization overvoltages in the circuit, especially at the open-end due to the Ferranti effect, and to minimize the capacitive current in the line breaker. These benefits cannot be achieved when shunt reactors are connected to busbars or to tertiary windings of power transformers at substations [20].

The installation of separate breakers for the shunt reactors results in an added switching flexibility as well as minimizing the risk of open phase resonance by decoupling reactors from the disconnected phase(s). If reactors remain connected to the disconnected phase(s), resonance may occur between the reactor inductance, inter-phase/inter-circuit capacitance, and the cable capacitance [21], [22].

Table II presents the lengths of the OHL and cable sections in each cable scenario reported in Table I. The defined section lengths are unequal since an asymmetrical mixed-line configuration is a more realistic assumption than a symmetrical one in which the circuit is identical at the two sides of the mid-point. Usually, realization of a completely symmetrical mixed-line configuration is difficult due to the practical limitations.

Table III presents the required shunt compensation size for each cable scenario. These values were obtained by a steady-state analysis presented in [20], which is based on the proposed method in [23]–[25]. SR1 and SR2 refer to the three-phase shunt reactors at the sending-end and receiving-end of the circuit, respectively, and the reported value for each of them is the total three-phase size. K_{sh} is the shunt compensation degree and shows the percentage of the cable reactive power compensated by the shunt reactors.

C. Grid Modeling

The time-domain simulations were carried out in the frequency-dependent model of the whole Dutch 380 kV transmission system in PSCAD/EMTDC. This model represents the entire Dutch 380 kV grid with frequency-dependent models to ensure the maximum simulation accuracy.

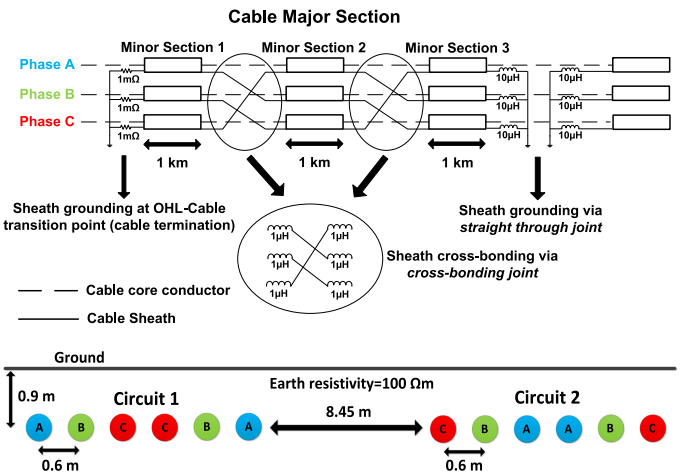

Fig. 2. Sheath cross-bonding and cable layout in the trench.

This model includes detailed representations of 380 kV substations, transmission lines, and three-phase three-limb power transformers, where the core saturation and parasitic capacitances of transformers are also included. The shunt reactors are represented by a multi-layer model and 380 kV capacitor banks by equivalent RLC circuits. The detailed explanations on the modelling of transformers and shunt reactors are available in [26]. The capacitor banks exist at some substations for voltage control and they are switched-in/out depending on the load-flow and voltage level. Equivalent parallel RL or RC loads were used for the representation of the lower voltage levels (220 kV and below).

In this model, OHLs and XLPE cables are represented by the frequency-dependent phase model of PSCAD, which is based on the Universal Line Model theory [27]. The input data of the model is based on the actual geometry and material properties of the represented transmission lines. The parameters used for the hybrid circuit under study can be found in [19]. The cable is single-core 2500 mm^2 copper conductor with XLPE insulation.

Fig. 2 illustrates the cable sheath cross-bonding and cable layout in the trench. It was assumed that the cable sections are composed of minor sections with the length of 1 km each. The screen conductors are cross-bonded at the end of each minor section (every 1 km) and they are grounded at the ends of each major section, which is made of three minor sections. A detailed model of each cross-bonding was applied in the Dutch grid model as a discrete representation of each minor section is the most accurate way of modelling [28]. The bonding wire and grounding impedance are represented by 1 μH inductances for cross-bonding joints, 10 μH inductances for groundings at straight through joints (connection of two major sections), and 1 mΩ resistances for groundings at cable terminations [29].

III. Statistical Behavior of Circuit-Breaker

The breaker closing time (T_{close}) is the instant when the breaker connects a phase to the voltage source and it can be expressed as follows [6], [14]:

$$T_{\mathrm{close}} = T_{\mathrm{command}} + \underbrace{\Delta T_{\mathrm{known}} + \Delta T_{\mathrm{stochastic}}}_{\Delta T_{\mathrm{operating}}} \qquad (1)$$

where T_{command} is the instant at which the breaker receives the closing command and $\Delta T_{\mathrm{operating}}$ is the breaker operating time representing the required time for the control and mechanical parts of the breaker to operate. $\Delta T_{\mathrm{known}}$ is the known and predictable part of the operating time (from measurements and/or adaptive control) and $\Delta T_{\mathrm{stochastic}}$ is the unpredictable variation in the operating time indicating the randomness of the closing time.

$\Delta T_{\mathrm{stochastic}}$ can be different between the poles due to the separate mechanical systems and it has a random behavior according to the normal distribution [6]–[17], [19]. The stochastic variations (inherent scatter) of the operating time can result in energization of phases at different instants, known as the pole closing span.

With regards to (1), the statistical behavior of the breaker closing time can be represented if two parameters are determined: (1) mean closing time, T_{mean}, where $T_{\mathrm{mean}} = T_{\mathrm{command}} + \Delta T_{\mathrm{known}}$, (2) pole closing span or distribution of pole closing times around the mean closing time ($\Delta T_{\mathrm{stochastical}}$). A sufficient number of these two parameters should be simulated to obtain accurate energization overvoltage distributions [14], [17], [30].

IV. Statistical Simulation Approach

The statistical analysis of energization overvoltages is more accurate when a larger number of switching times are simulated, but this requires a long computation time especially when a big and complex grid is modelled. For instance, each single switching simulation in the PSCAD model of the Dutch 380 kV grid can take up to a few hours to be completed depending on the simulated cable length. Such a long simulation time is mainly caused by the small numerical integration time step ($\Delta t = 4.8$ μs) and a large number of cables.

In [9]–[11], 100 random line energizations were performed to produce the overvoltage distributions, whilst the analysis was conducted in [12] by 200 random line energization cases. Literature has recommended minimum 100 simulations to obtain a sufficiently accurate overvoltage distribution [14], [17], [19], [30]. In this paper, 400 energizations were carried out for each study case to maximize the accuracy of the obtained statistical distributions. The applied approach for the selection of T_{mean} and the pole closing span is illustrated in Fig. 3:

1. T_{mean}*:* it was assumed that the breakers of the line and shunt reactors receive the closing command simultaneously and they have the same T_{mean}. The mean closing time can be any point of the power-frequency voltage cycle. 100 random points (with uniform distribution) were chosen by using the multiple-run feature of PSCAD.
2. *Pole closing span:* for each T_{mean}, 4 sets of pole closing span were simulated for each breaker. The pole span was determined by a random number generator using the normal (Gaussian) distribution. The mean value of the normal distribution was T_{mean} and the standard deviation was 1 ms ($\sigma = 1$ ms). The normal distribution curve was truncated at -3σ and $+3\sigma$.

The phase-peak method was applied to obtain the overvoltage probability distribution for each study case [3]. This means that from each energization simulation, the peak value of the phase-

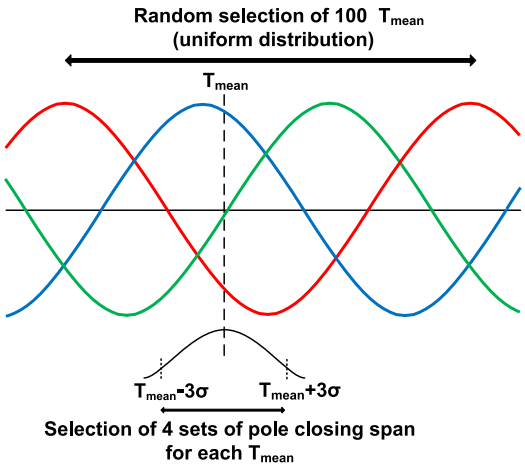

Fig. 3. Statistical variation of the breaker closing time over a cycle of the power-frequency voltage.

to-earth overvoltage on each phase at the point of interest was included in the overvoltage probability distribution. Therefore, the representative probability distribution for each case has 1200 overvoltage peak values (3 peak values per simulation × 400 simulations).

V. Simulation Results and Analysis

The no-load energization overvoltages of the hybrid circuit were simulated while it was energized from substation A and was open at the other side (see Fig. 1). The effects of cable length, shunt compensation size/location, short cable sections, short-circuit power, trapped charges, and mixed-line configuration on overvoltages were studied.

Throughout the paper, the point of interest is always the line open-end, unless a different location is mentioned. The overvoltages are expressed in per unit, where the base value (1 pu) is the peak value of the phase-to-ground nominal voltage (310.27 kV). Surge arresters are not modelled so that the worst overvoltages can be simulated.

The power-frequency and the transient voltages are the two components of the total switching overvoltage, so the obtained maximum overvoltages depend on the power-frequency voltage, which is here 1.076 pu (333.85 kV phase-to-ground). The short-circuit power at the substation from which the hybrid circuit is energized (substation A) is 26.3 GVA (corresponding to 37.14 kA fault current or 20 mH equivalent source inductance calculated at 408.88 kV $= (333.85\ \text{kV} \times \frac{\sqrt{3}}{\sqrt{2}})$.

A. Effect of Cable Length

The statistical switching analysis was performed on the six cable scenarios presented in Table I to find the influence of cable length on the distribution of energization overvoltages. Fig. 4 shows the obtained maximum overvoltages at the sending-end, open-end and all the six OHL-Cable transition points (TP). The fully-OHL and fully-cable scenarios are excluded since the transition points do not exist for these scenarios. It can be seen that for each cable scenario the maximum overvoltage becomes higher at transition points closer to the open-end as the highest overvoltage is at the open-end.

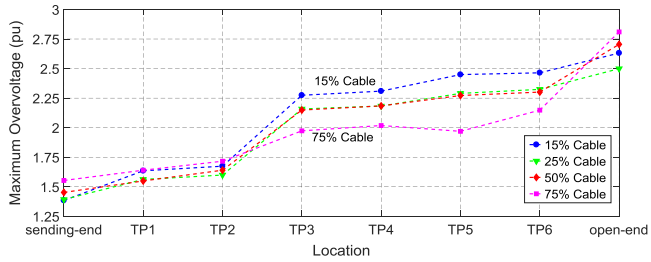

Fig. 4. Maximum energization overvoltage at different locations along the hybrid OHL-Cable circuit.

TABLE IV
Key Values of the Overvoltage Distributions

Scenario	Overvoltage (pu)			
	Max.	Mean	Stand. dev.	2% value
Fully OHL	2.826	1.821	0.358	2.509
15% Cable	2.631	1.756	0.262	2.346
25% Cable	2.499	1.694	0.245	2.269
50% Cable	2.705	1.689	0.259	2.319
75% Cable	2.810	1.626	0.256	2.329
Fully Cable	1.908	1.501	0.163	1.820

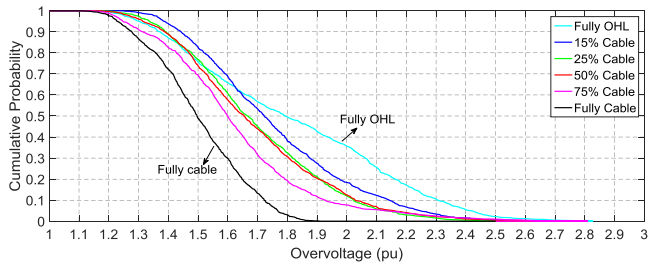

Fig. 5. Cumulative probability distributions of energization overvoltages of the six cable scenarios.

Table IV presents the maximum, mean, standard deviation, and 2% values, which are the four key values of the statistical distributions. The 2% value is the overvoltage value that the probability of this value being exceeded is 2% and is used for insulation coordination studies [3].

The complementary cumulative distribution functions (here called cumulative probabilities) of energization overvoltages of the six cable scenarios are given in Fig. 5. For a given overvoltage on the horizontal axis, the corresponding value on the vertical axis shows the probability that overvoltages exceed the given overvoltage.

As it is shown in Table IV, for the fully-OHL scenario, the maximum overvoltage (2.826 pu), mean overvoltage (1.821 pu), and 2% value (2.509 pu) are the highest among all the scenarios. In contrast, the lowest values are for the fully-cable circuit with the maximum overvoltage, mean overvoltage, and 2% value of 1.908, 1.501, and 1.820 pu, respectively. The standard deviation is also largest for the fully-OHL circuit and smallest for the fully-cable circuit. In addition, in Fig. 5, the probability of overvoltages is the highest for the fully-OHL circuit (for overvoltages above 1.65 pu), whereas it is always the lowest for the fully-cable circuit. These findings coincide with the con-

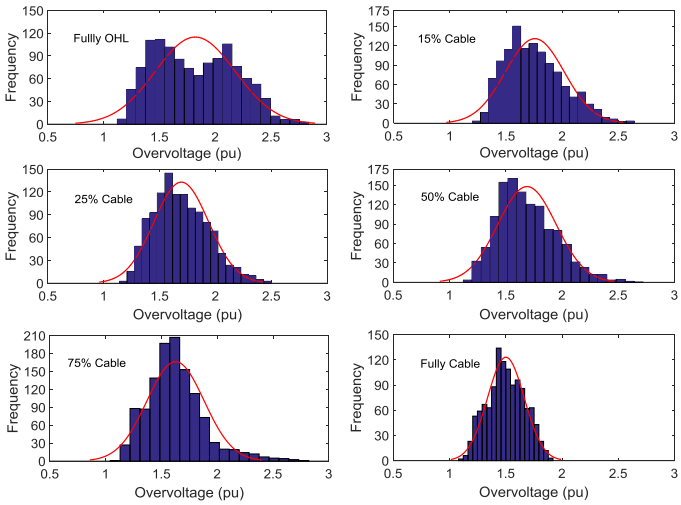

Fig. 6. Probability distributions of energization overvoltages of the six cable scenarios with fitted normal distribution curves.

TABLE V
SKEWNESS AND KURTOSIS OF THE ENERGIZATION OVERVOLTAGE DISTRIBUTIONS

Scenario	Skewness	Kurtosis
Fully OHL	0.239	2.084
15% Cable	0.581	2.867
25% Cable	0.453	2.802
50% Cable	0.640	3.262
75% Cable	1.012	4.886
Fully Cable	0.016	2.321

clusions of [12] and [13] that line energization overvoltages in cables are lower than those in OHLs.

According to Table IV, the hybrid scenarios produce overvoltages lower than those of the fully-OHL circuit and higher than those of the fully-cable circuit. The mean overvoltage decreases by increasing the cable length in the hybrid circuit, but the maximum overvoltage can decrease or increase depending on the cable scenario. Moreover, in Fig. 5 and for overvoltages above 1.65 pu, the overvoltage probabilities of the hybrid scenarios are between those of the fully-OHL and fully-cable circuits.

It can be concluded form the statistical simulations that a partial or full replacement of an overhead transmission line with cables results in lower energization overvoltages. It should be noted that for partial cabling cases this conclusion is a rule of thumb and may not be always valid due to its dependency on the system topology and parameters (e.g., see Sections V-D, V-E, and V-G for three exception examples).

The probability distributions of energization overvoltages of the six cable scenarios with fitted normal distribution curves are shown in Fig. 6. The probability distributions of random energization cases are usually compared to the normal distribution. The y-axis (height of rectangle) is the frequency with which the overvoltages in the specified range (width of rectangle) have occurred. Table V presents the skewness and kurtosis values of the overvoltage distributions.

The skewness is a measure describing how symmetrically the data are distributed around the mean value. The skewness of any symmetric distribution like the normal distribution is zero. A negative skewness indicates that the data has a longer tail to the left side of the mean value and a positive skewness indicates that the data has a longer tail to the right side. The overvoltage probability distributions of all the scenarios have positive skewness and are spread out more to the right side of the mean values. The fully-cable scenario has the smallest skewness indicating that its overvoltages probability distribution is the most symmetrical one.

The kurtosis is a measure of how outlier-prone (heavy- or light-tailed) a distribution is. Higher kurtosis indicates that the distribution is more outlier-prone (heavier-tailed) and lower kurtosis indicates that the distribution is less outlier-prone (lighter-tailed). The kurtosis of the normal distribution is 3. According to Table V, the fully-OHL scenario with the kurtosis of 2.084 is the less outlier prone scenario.

It has been observed that the energization overvoltages can substantially change when the share of cable in the circuit is varied. To interpret the simulation results, the significant physical differences between cables and OHLs, which influence the energization overvoltages, should be discussed.

The first difference between cables and OHLs is the propagation velocity and the behavior of the modal waves. According to the modal decomposition theory, a cross-bonded three-phase single-core cable system can be decomposed into six modes: one coaxial mode, two inter-phase modes, two inter-sheath modes, and one ground mode (in contrast to only one inter-phase mode and one earth-return mode for an OHL). Each mode has its own attenuation constant and propagation velocity [28], [31]–[33]. The wave propagation velocity in cables is much lower than that of OHLs as the coaxial mode is the fastest with the propagation velocity of $\frac{C_0}{\sqrt{\varepsilon_r\ \mu_r}}$ m/s, where ε_r and μ_r are respectively the relative permittivity and permeability (compared to $C_0 = 3 \times 10^8$ m/s for OHLs). For a typical cable, the propagation velocity is approximately between 1.6×10^8 to 1.8×10^8 m/s. If a cable is cross-bonded, the propagation velocity is slightly lower than these values [33].

During transients when an energizing wave propagates into the cable core conductor, all the six modal waves are excited and propagate toward the open-end while they reflect and refract at every impedance discontinuity point (impedance mismatch point), where the line surge impedance changes. Therefore, the resulting overvoltage at a given location on the circuit is the superimposition of all the modal waves at that location. As it is discussed in [13], the maximum energization overvoltage at the cable open-end is determined by the superimposition of the inter-phase mode (as the dominant mode) and the coaxial mode (as the superimposed mode), where the cycle time of the inter-phase mode (dominant mode) is dependent on the short-circuit power and the cable length. The overvoltages of the coaxial mode are low (compared with those of the inter-phase mode in OHLs) and also the cycle time of the inter-phase mode in cables is generally long. These two factors result in lower energization overvoltages for cables compared to OHLs.

The second difference between cables and OHLs is the existence of cross-bonding points for cables, which makes it more difficult for the waves to propagate to the open-end [12]. Furthermore, the third difference is the smaller surge impedance of

cables compared to that of OHLs, leading to lower overvoltages in cables for a same switching surge current [12], [34].

In addition to the mentioned differences between cables and OHLs, explanation about the reflection and refraction of the propagating waves in hybrid OHL-Cable circuits is also useful for interpretation of the simulation results. When an electromagnetic wave propagating along a hybrid circuit arrives to an impedance discontinuity point (sheath cross-bonding joints and OHL-Cable transition points), a part of the incident wave is reflected back and a part of the wave is transmitted beyond the point. The reflected voltage wave (V_R) and the transmitted voltage wave (V_T) can be calculated by the following equations [35]:

$$V_R = \frac{Z_2 - Z_1}{Z_2 + Z_1}.V \tag{2}$$

$$V_T = \frac{2Z_2}{Z_2 + Z_1}.V \tag{3}$$

where, V is the incident voltage wave, Z_1 is the surge impedance of the first transmission line through which the incident wave is traveling, and Z_2 is the surge impendence of the second transmission line.

In the case study project, the surge impedances of the OHLs and cables are around 220 Ω and 50 Ω, respectively. So, according to (2) and (3), when a voltage wave traveling through an OHL section reaches a transition point to a cable section, about 63% of the wave is reflected back with the negative polarity (with respect to the incident wave) and about 37% of the wave is transmitted to the cable. In contrary, when a wave traveling through a cable section reaches a transition point to an OHL section, about 63% of the wave is reflected back into the cable with the positive polarity (with respect to the incident wave) and 163% of the wave is transmitted to the OHL.

When a circuit consists of cascade connection of several OHL and cable sections, like the case study project, the propagating switching surge produces reflected and transmitted waveforms at all the impedance discontinuity points. This leads to a very complex propagation pattern, which can be analyzed by a lattice diagram. In this situation, the voltage at a given point on the circuit is determined by the superimposition of all the waves at every instant of time. The highest overvoltages occur when the best condition in terms of the system topology and parameters (e.g., number and location of sections and short-circuit power) are provided for the superposition of the waves.

B. Effect of Compensation Size

The shunt reactors are generally sized and located based on a steady-state analysis to control the power-frequency voltage and the capacitive current in the line breakers [20]. To deduce the impact of shunt reactors on the statistical distribution of energization overvoltages, the statistical analysis was conducted without shunt compensation and the results were compared with those of the shunt compensated circuit.

Table VI presents the key values of the overvoltage distributions and Fig. 7 shows the cumulative probabilities of energization overvoltages without and with shunt compensation. In all the cable scenarios, except the fully-cable scenario, the maximum overvoltage and the 2% value are lower when the circuit is energized without shunt compensation. In addition, for these scenarios, the probability of high overvoltages (above 1.7 pu) is lower when the circuit is energized without shunt compensation, although the post-switching steady-state overvoltages will be higher due to the Ferranti effect. This could be due to the superposition of the energization transients of the reactors and line when they are energized together.

TABLE VI
KEY VALUES OF THE OVERVOLTAGE DISTRIBUTIONS WITHOUT SHUNT COMPENSATION (VALUES IN PARENTHESES ARE WITH SHUNT COMPENSATION)

Scenario	Overvoltage (pu)			
	Max.	Mean	Stand. dev.	2% value
15% Cable	2.418 (2.631)	1.748 (1.756)	0.240 (0.262)	2.267 (2.346)
25% Cable	2.393 (2.499)	1.676 (1.694)	0.217 (0.245)	2.144 (2.269)
50% Cable	2.355 (2.705)	1.699 (1.689)	0.215 (0.259)	2.153 (2.319)
75% Cable	2.134 (2.810)	1.653 (1.626)	0.185 (0.256)	2.024 (2.329)
Fully Cable	2.083 (1.908)	1.613 (1.501)	0.154 (0.163)	1.920 (1.820)

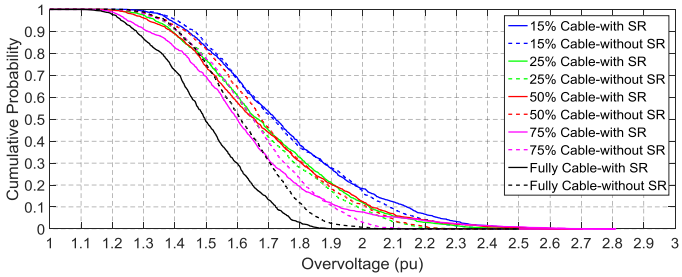

Fig. 7. Cumulative probability distributions of energization overvoltages with shunt compensation (solid lines) and without shunt compensation (dashed lines).

C. Effect of Compensation Location

The location of shunt reactors can be LEC (see Fig. 1) or distributed at multiple points along the route of the circuit. The technical convenience of the former or the latter has been assessed in [23] and [36], where the shunt compensation allocation for different study cases has been analyzed. The LEC is the most common scheme whereas the distributed techniques have multiple advantages over it; most notably, the increase of the available capacity for active power transfer and the need for a lower degree of compensation [20].

To deduce the influence of compensation location on the statistical distribution of energization overvoltages, overvoltages of a distributed compensation scheme in which reactors are located at each cable termination (OHL-Cable transition point) were compared with those of LEC. This type of compensation is called cable-end compensation (CEC). Therefore, instead of two reactor banks at two substations, six reactors banks (one at each cable termination) were considered with the sizes reported in [20].

Table VII presents the key values of the overvoltage distributions and Fig. 8 shows the cumulative probabilities of energization overvoltages with CEC and LEC. The key values and cumulative probabilities of overvoltages in all CEC scenarios

TABLE VII
KEY VALUES OF THE OVERVOLTAGE DISTRIBUTIONS WITH CEC
(VALUES IN PARENTHESES ARE WITH LEC)

Scenario	Overvoltage (pu)			
	Max.	Mean	Stand. dev.	2% value
15% Cable	2.413 (2.631)	1.708 (1.756)	0.245 (0.262)	2.245 (2.346)
25% Cable	2.255 (2.499)	1.648 (1.694)	0.214 (0.245)	2.117 (2.269)
50% Cable	2.288 (2.705)	1.639 (1.689)	0.219 (0.259)	2.095 (2.319)
75% Cable	2.046 (2.810)	1.568 (1.626)	0.194 (0.256)	1.952 (2.329)
Fully Cable	1.876 (1.908)	1.493 (1.501)	0.155 (0.163)	1.783 (1.820)

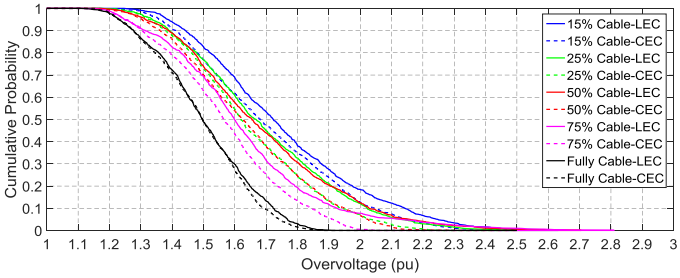

Fig. 8. Cumulative probability distributions of energization overvoltages with LEC (solid lines) and CEC (dashed lines).

are lower than those of the LEC scenarios, indicating another advantage of distributed compensation over the line-end compensation.

D. Effect of Short Cable Sections

In practice, short cable sections may be realized in a hybrid circuit. The short traveling time of the wave in short cable sections results in consecutive reflections and refractions at termination points leading to different overvoltages. To investigate this issue, six cases with short cable sections were defined for the 15% cable scenario. As illustrated in Fig. 9, the lengths of the OHL sections are unchanged in all the cases and only the lengths of the cable sections are varied while the total cable length is constant (12 km). Case 1 is the base case as defined in Table II. Cases 2, 3, and 4 have a 1 km-long cable section at the sending side, middle, and the receiving side of the circuit, respectively. Cases 5 and 6 have two 1 km-long cable sections at middle plus the sending or receiving sides.

The maximum overvoltages and the cumulative probabilities of energization overvoltages are respectively shown in Figs. 10 and 11. It can be observed that Case 6 has the highest maximum overvoltage (3.3 pu) and overvoltage probability among all the cases even higher than those of the fully-OHL scenario. On the contrary, Case 5 has the lowest maximum (2.44 pu) and probability of overvoltages. In addition, after Case 6, the highest maximum and probability of overvoltages are produced in Case 4.

It can be concluded that for a given cable scenario, the highest energization overvoltages are expected when very short cable sections are at the open-end of the circuit. For the studied cases, these overvoltages are up to 0.86 pu (equal to 267 kV) higher than those of the other cases. In contrast, the existence of longer

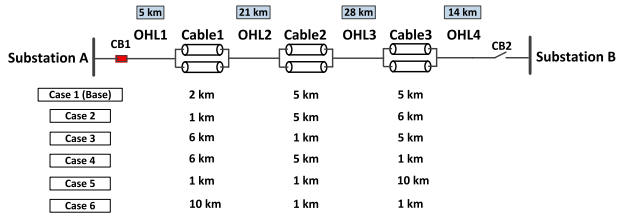

Fig. 9. Cases of short cable sections for the 15% cable scenario (lengths of the OHL sections are unchanged).

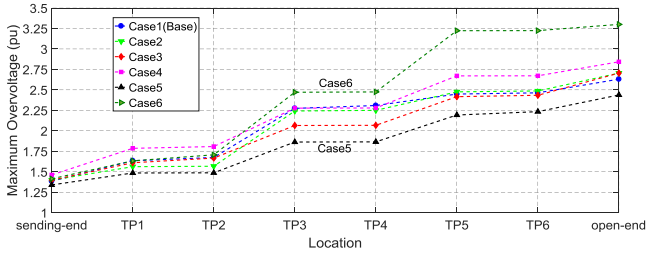

Fig. 10. Maximum energization overvoltage at different locations along the hybrid OHL-Cable circuit for the cases in Fig. 9.

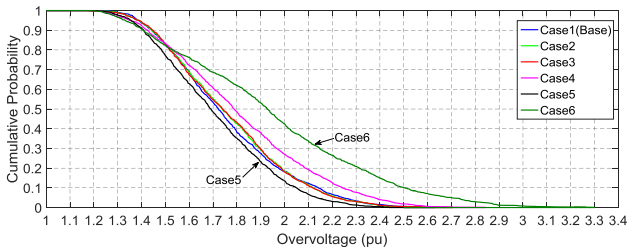

Fig. 11. Cumulative probability distributions of energization overvoltages of the cases in Fig. 9.

cable sections at the open-end results in lower overvoltages. This can be due to the short travelling time of the propagating wave in the short cable sections and the successive reflections and refractions.

E. Effect of Short-Circuit Power

The influence of the grid short-circuit power on the statistical distribution of energization overvoltages was studied by the use of an equivalent grid model consisting of the hybrid circuit and a lumped-parameter inductive source. In fact, the Thevenin equivalent was used instead of the whole grid model with distributed generation because it is more flexible and convenient to adjust the short-circuit power with the variation of the equivalent source impedance. A Frequency Dependent Network Equivalent (FDNE) can be also an option to represent the entire grid if it can properly represent the generation and short-circuit power of the grid [37].

In the equivalent model of the grid, the power-frequency voltage at the sending substation was adjusted to the same voltage in the whole grid model (1.076 pu). The statistical analysis was carried out for five source inductances of 15, 20, 25, 50, and 100 mH. The 20 mH source inductance is equal to the equivalent short-circuit inductance calculated at the sending substation in the whole grid model.

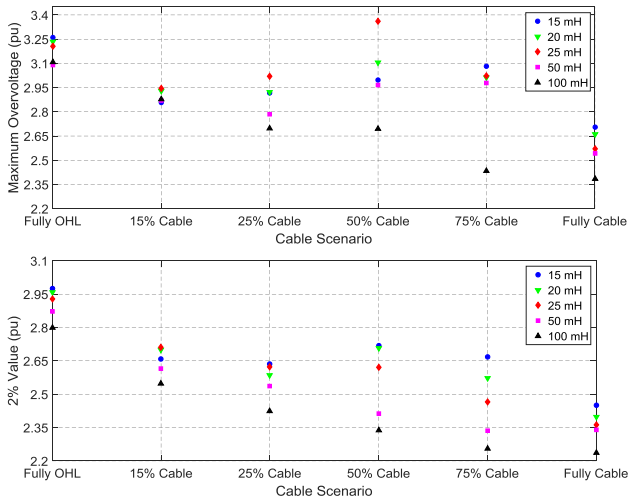

Fig. 12. Maximum energization overvoltage and 2% value for different feeding network short-circuit powers.

Fig. 12 shows the maximum energization overvoltage and 2% value for different feeding networks. For a given source inductance, the lowest and highest values are for the fully-cable and the fully-OHL scenarios, respectively. The only exception is the 50% cable scenario with 25 mH source inductance, for which the maximum overvoltage (3.36 pu) is higher than that of the fully-OHL circuit although the corresponding 2% value is still lower. In addition, for all source impedances, the hybrid scenarios produce overvoltages higher than those of the fully-cable scenario and very likely lower than those of the fully-OHL scenario. This conclusion coincides with those in the previous sections.

It can be also noticed that each cable scenario has a different behavior than the other scenarios when the short-circuit power is varied. For the fully-OHL scenario, the maximum overvoltage decreases when the source inductance increases from 15 mH to 50 mH and thereafter slightly increases for 100 mH; however, the 2% value always decreases with increasing the source impedance (weaker feeding networks). For the fully-cable scenario, both the maximum overvoltage and 2% value decrease by increasing the source impedance. For the hybrid scenarios, the dependency of overvoltages on the feeding network strength changes case-by-case.

As it was previously mentioned, the maximum energization overvoltage at the cable open-end is determined by superimposition of the inter-phase mode (as the dominant mode) and the coaxial mode (as the superimposed mode), where the cycle time of the inter-phase mode is dependent on the short circuit power and the cable length [13]. For larger source impedances (weaker feeding networks), the rate of rise of voltage is lower and the cycle time of the inter-phase mode (dominant mode) is longer. Thus, by the time when the inter-phase mode reaches its maximum at the open-end, the coaxial mode has travelled back and forth to the open-end for several times and has become highly damped. As a result, the energization overvoltage will be likely lower when the source impedance is larger (weaker feeding network).

TABLE VIII
KEY VALUES OF THE OVERVOLTAGE DISTRIBUTIONS WITH TRAPPED CHARGES (VALUES IN PARENTHESES ARE WITHOUT TRAPPED CHARGES)

Scenario	Overvoltage (pu)			
	Max.	Mean	Stand. dev.	2% value
15% Cable	3.319 (2.631)	1.763 (1.756)	0.275 (0.262)	2.380 (2.346)
25% Cable	2.788 (2.499)	1.702 (1.694)	0.257 (0.245)	2.289 (2.269)
50% Cable	2.849 (2.705)	1.695 (1.689)	0.273 (0.259)	2.388 (2.319)
75% Cable	2.780 (2.810)	1.614 (1.626)	0.254 (0.256)	2.330 (2.329)
Fully Cable	2.036 (1.908)	1.498 (1.501)	0.167 (0.163)	1.828 (1.820)

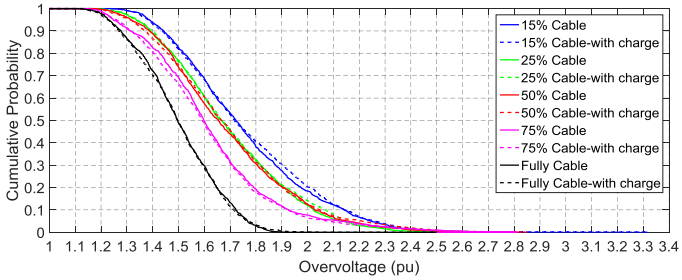

Fig. 13. Cumulative probability distributions of energization overvoltages without trapped charges (solid lines) and with trapped charges (dashed lines).

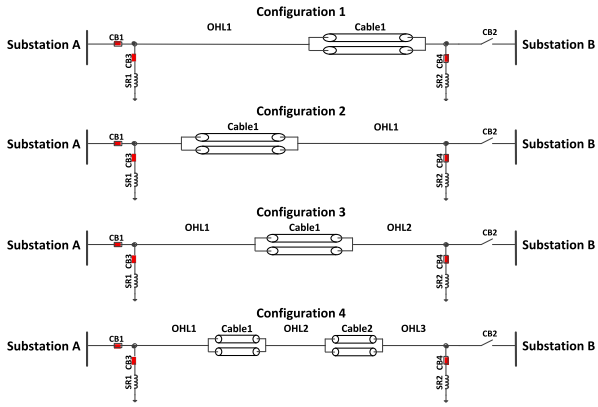

Fig. 14. Single-line diagram of the simulated mixed-line configurations.

The comparison of the simulated overvoltages of the whole grid model in Table IV with those of the equivalent model with 20 mH source inductance (as the corresponding inductance with the short-circuit power of the whole grid model) shows that the simulated overvoltages are higher in the equivalent grid. This is due to the fact that the actual damping and wave propagation to the rest of the grid are not represented by the equivalent model.

F. Effect of Trapped Charges

Trapped charges may exist on disconnected cables and result in very high overvoltages when the voltage of the trapped charges has opposite polarity to that of the switching surge [38]. The study was conducted by initial charging of the cables with three single-phase 30 kV dc voltage sources and then the statistical switching of the breakers whilst the dc sources are removed.

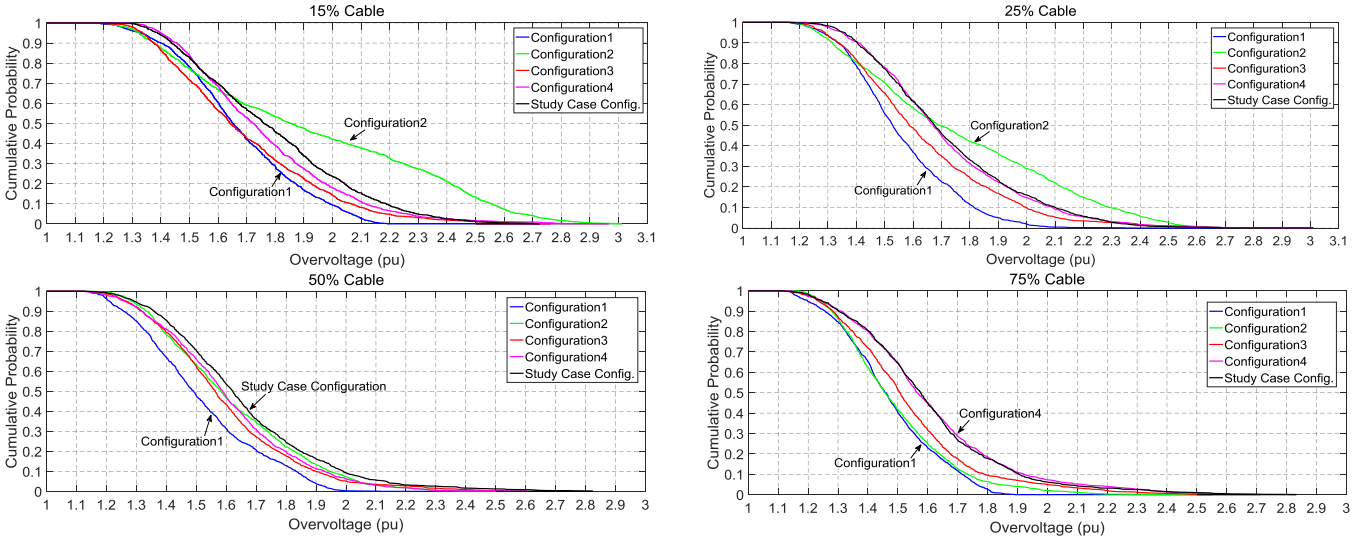

Fig. 15. Cumulative probability distributions of energization overvoltages for different mixed-line configurations.

Table VIII and Fig. 13 show the key values of the overvoltage distributions and the cumulative probability distributions, respectively. The maximum overvoltages are up to 0.68 pu higher than those of the cases without trapped charge, whereas the difference in 2% values is much less and only up to 0.07 pu. Moreover, the differences between the cumulative probabilities are negligible, indicating that generally overvoltages are not higher except for particular switching instants at which the resulting switching surge and trapped charges cause a very high overvoltage together. It should be noted that higher overvoltages can be expected if the residual voltage on the cables is higher than 30 kV.

G. Effect of Mixed-Line Configuration

It is also important to investigate the influence of mixed-line configuration on the statistical distribution of energization overvoltages. Different configurations can be derived by varying the number and location of the OHL and cable sections. In addition to the study case configuration in Fig. 1, four mixed-line configurations as shown in Fig. 14 were selected for the comparison. As it is concluded in [20], the required compensation size for each configuration is different, so the reported values in [20] were used for this study. In addition, for a given cable scenario and configuration, it was assumed that all the OHL sections are equally long and the same for all the cable sections.

The cumulative probabilities of energization overvoltages are shown in Fig. 15. For a given cable scenario, the difference between the cumulative probabilities of different configurations can be up to 35%. Therefore, the number and distribution of the OHL and cable sections can substantially affect overvoltages due to the consequent changes in the wave propagation pattern.

In addition, Configuration 1, in which a long cable section is at the open-end of the circuit, produces the lowest overvoltages for all the scenarios. This finding coincides with the conclusions of Section V.D. The reason that Configuration 1 produces lower overvoltages than the other configurations is as follows: when the traveling voltage wave through the OHL section reaches the transition point to the cable section, about 63% of the incident wave is reflected back (see (2) and (3)) and only 37% of the incident wave is transmitted to the cable and moving toward the open-end. So, the resulting overvoltage at the open-end of the circuit will be lowered.

VI. Conclusions

The statistical distribution of energization overvoltages plays an important role in determination of the required insulation levels for EHV components. In this paper, the distribution of energization overvoltages of hybrid OHL-Cable circuits was thoroughly studied by means of numerous statistical switching simulations.

It was discovered that a hybrid OHL-Cable circuit produces energization overvoltages higher than those of a fully-cable circuit and very likely lower than those of a fully-OHL circuit with the same transmission lengths. This means that the risk of experiencing high energization overvoltages and stressing system components is higher in a fully-OHL circuit than in a partial or fully undergrounded circuit.

Energization overvoltages are very dependent on the number, location, and lengths of the OHL and cable sections because of the consequent changes in the energizing wave propagation. For a given cable scenario, the existence of long cable sections at the open-end of the circuit results in lower energization overvoltages compared to the case that short cable sections are at the open-end. In addition, the difference between the overvoltage cumulative probabilities of different mixed-line configurations can be also substantial, where, as an example, it was up to 35% for the studied configurations in this paper. This shows the high impact of the number and distribution of the OHL and cable sections on energization overvoltages.

Furthermore, energization overvoltages can be substantially affected by the system parameters, most notably the short-circuit power of the feeding network and the shunt compensation size and location. The transient energization overvoltages will be likely lower when the network short-circuit power is lower (i.e.,

weaker feeding network), whereas the post-switching steady-state overvoltages will be higher due to the Ferranti effect at the open-end of the circuit. Moreover, a distributed reactive power compensation along the circuit, like CEC, results in lower overvoltages compared to the line-end compensation.

Finally, in specific situations, extremely high overvoltages may occur in hybrid OHL-Cable circuits, such as the presence of trapped charges on the cable, the existence of very short cable sections at the open-end of the circuit, and certain short-circuit powers. A special attention should be paid to these situations as they can lead to a component failure and/or exceeding the energy absorption capacity of surge arresters and sheath voltage limiters.

REFERENCES

[1] CIGRE Working Group C4.502, "Power system technical performance issues related to the application of long HVAC cables," CIGRE, Paris, France, Tech. Brochure 556, Oct. 2013.

[2] R. Benato and D. Napolitano, "State-space model for availability assessment of EHV OHL–UGC mixed power transmission link," *Elect. Power Syst. Res.*, vol. 99, pp. 45–52, 2013.

[3] Insulation Co-Ordination-Part 2: Application *Guide*, IEC Standard 60071-2, 1996.

[4] CIGRE Working Group 21/33, "Insulation co-ordination for HV AC underground cable systems," CIGRE, Paris, France, Tech. Brochure 189, Jun. 2001.

[5] A. R. Hileman, *Insulation Coordination for Power Systems*. New York, NY, USA: Marcel Dekker, Jun. 1999.

[6] R. Smeets, L. van der Sluis, M. Kapetanovic, D. Peelo, and A. Janssen, *Switching in Electrical Transmission and Distribution Systems*. Hoboken, NJ, USA: Wiley, 2015.

[7] ABB, Ludvika, Sweden, Live Tank Circuit Breakers: Buyer's Guide, 6th ed., 2014.

[8] CIGRE Working Group 13.02, "Switching overvoltages in EHV and UHV systems with special reference to closing and reclosing transmission lines," *Electra*, no. 30, pp. 70–122, 1973.

[9] CIGRE Working Group 13.05, "The calculation of switching surges," *Electra*, no. 19, pp. 67–78, 1971.

[10] CIGRE Working Group 13.05, "The calculation of switching surges-II. Network representation for energization and re-energization studies on lines fed by an inductive source," *Electra*, no. 32, pp. 17–42, 1974.

[11] CIGRE Working Group 13.05, "The calculation of switching surges-III. Transmission line representation for energization and re-energization studies with complex feeding networks," *Electra*, no. 62, pp. 45–78, 1979.

[12] T. Ohno, C. L. Bak, A. Ametani, W. Wiechowski, and T. K. Sørensen, "Statistical distribution of energization overvoltages of EHV cables," *IEEE Trans. Power Del.*, vol. 28, no. 3, pp. 1423–1432, Jul. 2013.

[13] T. Ohno, A. Ametani, C. L. Bak, W. Wiechowski, and T. K. Sørensen, "Analysis of the statistical distribution of energization overvoltages of EHV cables and OHLs," in *Proc. Int. Conf. Power Syst. Transients*, Vancouver, BC, Canada, Jul. 2013, pp. 1–7.

[14] P. Mestas and M. C. Tavares, "Relevant parameters in a statistical analysis-application to transmission-line energization," *IEEE Trans. Power Del.*, vol. 29, no. 6, pp. 2605–2613, Dec. 2014.

[15] A. H. Hamza, S. M. Ghania, A. M. Emam, and A. S. Shafy, "Statistical analysis of switching overvoltages and insulation coordination for a 500 kV transmission line," in *Proc. 18th Int. Middle East Power Syst. Conf.*, Cairo, Egypt, Dec. 2016, pp. 1–4.

[16] M. Z. Daud, P. Ciufo, and S. Perera, "Statistical analysis of overvoltages due to the energization of a 132 kV underground cable," in *Proc. 6th ECTI Conf.*, Pattaya, Thailand, May 2009, pp. 54–57.

[17] J. A. Martinez, R. Natarajan, and E. Camm, "Comparison of statistical switching results using Gaussian, uniform and systematic switching approaches," in *Proc. IEEE Power Eng. Soc. Summer Meeting*, Seattle, WA, USA, Jul. 2000, pp. 884–889.

[18] Y. Itoh, N. Nagaoka, and A. Ametani, "Transient analysis of a crossbonded cable system underneath a bridge," *IEEE Trans. Power Del.*, vol. 5, no. 2, pp. 527–532, Apr. 1990.

[19] H. Khalilnezhad, M. Popov, J. A. Bos, J. P. W. de Jong, and L. van der Sluis, "Investigation of statistical distribution of energization overvoltages in 380 kV hybrid OHL-cable systems," in *Proc. Int. Conf. Power Syst. Transients*, Seoul, South Korea, Jun. 2017, pp. 1–6.

[20] H. Khalilnezhad, S. Chen, M. Popov, J. A. Bos, J. P. W. de Jong, and L. van der Sluis, "Shunt compensation design of EHV double-circuit mixed OHL-cable connections," in *Proc. IET Int. Conf. Resilience Transmiss. Distrib. Netw.*, Birmingham, U.K., 2015, pp. 1–6.

[21] CIGRE Working Group C4.307, "Resonance and feroresonance in power networks," CIGRE, Paris, France, Tech. Brochure 569, Feb. 2014.

[22] H. Khalilnezhad, M. Popov, J. A. Bos, J. P. W. de Jong, L. van der Sluis, and A. Ametani, "Countermeasures of zero-missing phenomenon in (E)HV cable systems," *IEEE Trans. Power Del.*, vol. 33, no. 4, pp. 1657–1667, Aug. 2018.

[23] S. Lauria, F. M. Gatta, and L. Colla, "Shunt compensation of EHV cables and mixed overhead-cable lines," in *Proc. IEEE Power Technol. Conf.*, Lausanne, Switzerland, Jul. 2007, pp. 1344–1349.

[24] F. M. Gatta, A. Geri, S. Lauria, and M. Maccioni, "Steady-state operation conditions of very long EHVAC cable lines," *Elect. Power Syst. Res.*, vol. 81, pp. 1525–1533, 2011.

[25] R. Benato and A. Paolucci, *EHV AC Undergrounding Electrical Power: Performance and Planning*. Berlin, Germany: Springer, 2010.

[26] L. Wu, "Impact of EHV/HV underground power cables on resonant grid behavior," Ph.D. dissertation, Dept. Elect. Eng., Eindhoven Univ. Technol., Eindhoven, The Netherlands, Oct. 2014.

[27] Manitoba HVDC Research Centre, Winnipeg, MB, Canada, "User's guide on the EMTDC analysis for PSCAD power system simulation," 2010.

[28] I. Lafaia, J. Mahseredjian, A. Ametani, M. T. Correia de Barros, I. Kocar, and Y. Fillion, "Frequency and time domain response of cross-bonded cables," *IEEE Trans. Power Del.*, vol. 33, no. 2, pp. 640–648, Apr. 2018.

[29] U. S. Gudmundsdottir, B. Gustavsen, C. L. Bak, and W. Wiechowski, "Field test and simulation of a 400-kV cross-bonded cable system," *IEEE Trans. Power Del.*, vol. 26, no. 3, pp. 1403–1410, Jul. 2011.

[30] A. I. Ibrahim and H. W. Dommel, "A knowledge base for switching surge transients," in *Proc. Int. Conf. Power Syst. Transients*, Montreal, QC, Canada, 2005, pp. 1–6.

[31] F. F. da Silva and C. L. Bak, *Electromagnetic Transients in Power Cables*. London, U.K.: Springer, 2013.

[32] C. F. Jensen, U. S. Gudmundsdottir, C. L. Bak, and A. Abur, "Field test and theoretical analysis of electromagnetic pulse propagation velocity on crossbonded cable systems," *IEEE Trans. Power Del.*, vol. 29, no. 3, pp. 1028–1034, Jun. 2014.

[33] A. Ametani, T. Ohno, and N. Nagaoka, *Cable System Transients: Theory, Modeling and Simulation*. Singapore: Wiley, Jul. 2015.

[34] CIGRE Working Group B1.30, "Cable systems electrical characteristics," CIGRE, Paris, France, Tech. Brochure 531, Apr. 2013.

[35] A. Greenwood, *Electrical Transients in Power Systems*. Hoboken, NJ, USA: Wiley, 1971.

[36] R. Benato and A. Paolucci, "Operating capability of long AC EHV transmission cables," *Elect. Power Syst. Res.*, vol. 75, pp. 17–27, 2005.

[37] J. Morales, J. Mahseredjian, K. Sheshyekani, A. Ramirez, E. Medina, and I. Kocar, "Pole-selective residue perturbation technique for passivity enforcement of FDNEs," *IEEE Trans. Power Del.,* vol. 33, no. 6, pp. 2746–2754, Dec. 2018.

[38] F. Ghassemi, "Effect of trapped charges on cable SVL failure," *Elect. Power Syst. Res.*, vol. 115, pp. 18–25, 2014.

Hossein Khalilnezhad (GSM'12) was born in Iran in 1987. He received the B.Sc. degree in electrical engineering from the Shiraz University of Technology, Shiraz, Iran, and the M.Sc. degree (*cumlaude*) in electrical power engineering from the Delft University of Technology, Delft, The Netherlands, in September 2013. He is currently working toward the Ph.D. degree at the Delft University of Technology, where he studies EHV underground cable systems. He was the recipient of the Shell Master Award for the best M.Sc. thesis in the field of innovation and technology in March 2014 and the IEEE PES Travel Grant at the POWERCON Conference in Australia in September 2016.

Marjan Popov (M'95–SM'03) received the Dipl.Ing. degree from the University of Skopje, Skopje, Republic of Macedonia, in 1993, and the Ph.D. degree in electrical power engineering from Delft University of Technology, Delft, The Netherlands, in 2002. In 1997, he was an Academic Visitor with the University of Liverpool, working with the Arc Research Group on modeling SF6 circuit breakers. He is an Associate Professor with the Department of Electrical Sustainable Energy, Delft University of Technology. His research interests include future power systems, large scale of power system transients, intelligent protection for future power systems, and wide area monitoring and protection. He is also an Associate Editor for Elsevier's *JEPES*. He is a member of CIGRE and actively participated in Working Group C4.502 and Working Group A2/C4.39. He was the recipient of the prestigious Dutch Hidde Nijland Award in 2010, the IEEE PES Prize Paper Award, and the IEEE Switchgear Committee Award in 2011.

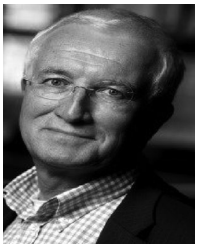

Lou van der Sluis (M'81–SM'86–LSM'16) was born in Geervliet, The Netherlands, in 1950. He received the M.Sc. degree in electrical engineering from the Delft University of Technology, Delft, The Netherlands, in 1974. He joined the KEMA High Power Laboratory in 1977 as a Test Engineer. In 1990, he became a part-time Professor and since 1992, he has been a full-time Professor with the Department of Power Systems, Delft University of Technology. He has authored *Transients in Power Systems* and coauthor of *Electrical Power System Essentials* and *Switching in Electrical Transmission and Distribution Systems*. He is a past Convener of CC-03 of CIGRE and CIRED. He has been a member of CIGRE WG A3-24 on internal arc testing and a member of CIGRE WG C4-502 to study the interaction between high-voltage overhead lines and underground cables. He is a member of the advisory board of SC-A3 of CIGRE.

Jorrit A. Bos received the M.Sc. degree in electrical engineering from the Delft University of Technology, Delft, The Netherlands, in 2008. In 2008, he joined TenneT TSO as a Technical Trainee in the young professional program, where he worked in three different departments. Since 2010, he has been a Grid Strategist with the Department of Grid Development of TenneT. He currently holds the position of Senior Grid Strategist for the 150 kV grid developments in the southern part of the Netherlands. His research interests include European grid development within the North Sea region, 380 kV cable research, and dynamic stability analysis.

Akihiro Ametani (M'71–SM'83–F'92–LF'10) received the Ph.D. degree in power system transients from the Institute of Science and Technology (UMIST), University of Manchester, Manchester, U.K., in 1973, and the D.Sc. degree (higher degree in U.K.) from the University of Manchester, Manchester, U.K., in 2010. From 1971 to 1974, he was with the UMIST and Bonneville Power Administration, Portland, OR, USA, and developed an Electromagnetic Transients Program for Summers 1976 to 1981. Since 1985, he has been a Professor with Doshisha University, Kyoto, Japan, and was a Professor with the Chatholic University of Leaven, Leuven, Belgium, in 1988. He was the Director of the Institute of Science and Engineering from 1996 to 1998, and the Dean of Library and Computer/Information Center, Doshisha University, from 1998 to 2001. He was the Vice-President of the Institute of Electrical Engineers of Japan in 2003 and 2004. He is a Chartered Engineer in the U.K., a Fellow of IET, and a distinguished member of CIGRE.